Send Orders for Reprints to reprints@benthamscience.net

Current Pharmaceutical Design, XXXX, *XX*, 1-14

RESEARCH ARTICLE

Deformable Vesicles with Edge Activators for the Transdermal Delivery of Non-Psychoactive Cannabinoids

Elisa Vettorato[1,*], Marisa Fiordelisi[1], Silvia Ferro[1], Desiré Zanin[1], Erica Franceschinis[1], Giovanni Marzaro[1] and Nicola Realdon[1]

[1]*Department of Pharmaceutical and Pharmacological Sciences, University of Padova, Via F. Marzolo, 5, Padova 35131, Italy*

ARTICLE HISTORY

Received: October 30, 2023
Accepted: January 22, 2024

DOI:
10.2174/0113816128289593240226071813

Abstract: ***Background*:** Transdermal delivery of highly lipophilic molecules is challenging due to the strong barrier function of the skin. Vesicles with penetration enhancers are safe and efficient systems that could improve the transdermal delivery of non-psychoactive cannabinoids such as cannabidiol and desoxy-cannabidiol. In the last decades, research interest in desoxy-cannabidiol as a potent drug with anti-nociceptive properties has risen. Still, its scarce market availability poses a limit for both research and clinical applications. Therefore, it is necessary to improve the synthesis to produce sufficient amounts of desoxy-cannabidiol. Moreover, also the formulation aspects for this drug are challenging and require to be addressed to meet an efficient delivery to the patients.

***Objective*:** This work aimed to develop innovative phospholipid-based vesicles with propylene glycol (PG), oleic acid (OA), or limonene as edge activators, for the transdermal delivery of highly lipophilic drugs such as non-psychoactive cannabinoids. In particular, desoxy-cannabidiol was selected thanks to its anti-nociceptive activity, and its synthesis was improved enhancing the stereoselectivity of its synthon's production.

***Methods*:** Desoxy-cannabidiol was synthesized by Lewis acid-mediated condensation of *p*-mentha-2,8-dien-1-ol and *m*-pentylphenol, improving the stereoselectivity of the first synthon's production. Transethosomes containing 20-50% w/w PG, 0.4-0.8% w/w OA, or 0.1-1% w/w limonene were optimized and loaded with cannabidiol or desoxy-cannabidiol (0.07-0.8% w/w, 0.6-7.0 mg/mL). *Ex-vivo* studies were performed to assess both the skin permeation and accumulation of the cannabinoids, as well as the penetration depth of fluorescein-loaded systems used as models.

***Results*:** An enantioselective bromination was added to the pathway, thus raising the production yield of *p*-mentha-2,8-dien-1-ol to 81% against 35%, and the overall yield of desoxy-cannabidiol synthesis from 12% to 48%. Optimized transethosomes containing 0.6 mg/mL cannabinoids were prepared with 1:10 PG:lipid weight ratio, 0.54 OA:lipid molar ratio, and 0.3 limonene:lipid molar ratio, showing good nanometric size (208 ± 20.8 nm - 321 ± 26.3 nm) and entrapment efficiency (> 80%). *Ex-vivo* tests showed both improved skin permeation rates of cannabinoids (up to 21.32 ± 4.27 μg/cm^2 cannabidiol), and skin penetration (depth of fluorescein up to 240 μm, with PG).

***Conclusion*:** Desoxy-cannabidiol was successfully produced at high yields, and formulated into transethosomes optimized for transdermal delivery. Loaded vesicles showed improved skin penetration of desoxy-cannabidiol, cannabidiol and a lipophilic probe. These results suggest the potential of these carriers for the transdermal delivery of highly lipophilic drugs.

Keywords: Desoxy-cannabidiol, cannabidiol, skin, phospholipids, vesicles, propylene glycol, oleic acid, limonene.

1. INTRODUCTION

Deformable vesicles for enhanced skin delivery of lipophilic drugs have been extensively studied in the last decades. Dermal application of rigid liposomes and non-phospholipidic vesicles caused drug accumulation in the *Stratum corneum* (SC), the outmost layer of the skin [1-3]. Instead, innovative phospholipid-based systems have been developed to efficient

ly deliver drugs to the dermis and the deepest skin layers [4]. By introducing an edge activator (EA) into the phospholipid layers, *i.e.*, a membrane softening agent, it was possible to produce highly deformable and elastic vesicles such as transfersomes (single-chain surfactants-containing liposomes) and invasomes (terpenes-containing liposomes). Both systems are typically produced by thin-film hydration method, and their components were reported to disrupt the SC tight lipid packing, thus significantly improving the penetration of lipophilic drugs across the skin [5-11]. Around the 2000s, Touitou developed the ethosomes: soft, deformable vesicles composed of phospholipids and high concentrations of short-chain alcohols (mainly ethanol), prepared by aqueous phase injection under fast mixing [12]. The high alcoholic concentrations fluidize the phospholipidic layers, leading to smaller, homogenous, and more deformable systems than rigid liposomes obtained by the film-forming method [12, 13]. By adding penetration enhancers or EAs, transethosomes were obtained and first reported in 2012 [14]. Dif-

*Address correspondence to this author at the Department of Pharmaceutical and Pharmacological Sciences, University of Padova, Via F. Marzolo, 5, Padova 35131, Italy; E-mail: elisa.vettorato@phd.unipd.it

1381-6128/XX $65.00+.00

ferent EAs have been investigated to improve the features of ethosomal systems, from fatty acids to sulfoxides derivatives, leading to enhanced skin penetration of lipophilic drugs such as voriconazole and 5-fluorouracil [14-16].

In this study, ethosomes were prepared with a short-chain glycol, such as propylene glycol (PG). At the same time, transethosomes were formulated with a single-chain fatty acid (oleic acid, OA), or the terpene R-(+)-limonene. Propylene glycol (PG) is a safe and widely used co-solvent for skin delivery which can fluidize phosphatidylcholine (PC) layers, improving both the skin delivery of drugs and the vesicles' properties [13, 17-19]. OA is a C18 *cis*-9 monounsaturated fatty acid and a skin penetration enhancer as such [20, 21], although better tolerated when incorporated in liposomes, as the dielectric effect of the non-polar lipid membrane partially shields the negative charges [22-24]. OA showed a synergic skin penetration activity when combined with phospholipidic vesicles up to the critical molar ratio of 0.67 [22, 25-29]. Terpenes are small, lipophilic molecules that lower the transition temperature of lipids and phospholipids, thus causing rearrangements of membranes and reducing the lipids packing according to the unsaturation degree of the hydrophobic tails, up to a 1:4 terpene:lipid molar ratio [30-32].

Ethosomes and transethosomes proved high efficiency in the skin delivery of highly lipophilic drugs [33, 34]. In the present study, two lipophilic cannabinoids were formulated: cannabidiol (CBD), the widely known phytocannabinoid with a pharmacological activity as an anti-epileptic in severe, drug-resistant syndromes and an anti-inflammatory agent [35-38]; and desoxy-cannabidiol (DH-CBD). Although similar in their terpene-phenolic structure, their aromatic cores differ in the hydroxyl group, leading to a decreased affinity of DH-CBD towards the cannabinoids receptors (Fig. **1**). Since this property has gained interest in the scientific community, DH-CBD is currently under investigation as a selective agonist of inhibitory glycine receptors, which play a key role in regulating neuromotor activity, pain sensation, muscle relaxation, and anxiety [39-43]. However, to date, DH-CBD is not easily affordable and scarcely available. Reggio first proposed its total synthesis as a condensation of *p*-mentha-2,8-dien-1-ol and *m*-pentylphenol *via* DMF-dineopental acetal [44, 45], and limited alternatives were suggested in further studies [46, 47]. Wilkinson *et al*. in 2013 reported a novel approach to obtain *p*-mentha-2,8-dien-1-ol by Cope elimination from R-(+)-limonene oxide, and a final coupling with *m*-pentylphenol using boron trifluoride, resulting in a slightly higher efficiency than in the previously mentioned synthetic pathways [39, 45, 48]. While improving the total synthetic pathway, the reaction yield was still limited by the low stereoselectivity in the production of the *p*-mentha-2,8-dien-1-ol synthon. This study proposes a further improvement in the stereoselectivity by introducing an additional step in the *p*-mentha-2,8-dien-1-ol synthesis.

While the clinical efficacy of CBD and DH-CBD is recognized, efficient delivery to the patient is often an unmet need because of high variability in the absorbed dose [49, 50]. Transdermal delivery of cannabinoids could allow a constant release of these drugs, with a sustained dosage over a prolonged time. Since both cannabinoids display high lipophilicity with a calculated LogP ~6 [51], they tend to accumulate in the SC without reaching the deeper strata and the bloodstream [21, 52]. For this reason, their skin permeation must be enhanced by efficient skin delivery systems. To overcome these limitations, topical transdermal formulations have been developed with adequate skin penetration enhancement of Δ^9-tetrahydrocannabinol and CBD [13, 35, 52-55]. To the best of our knowledge, no transdermal systems have been developed for the delivery of DH-CBD to date. In addition, in this work ethosomal-like vesicles containing PG as a co-solvent were compared to innovative transethosomal systems with OA or R-(+)-limonene and validated with *ex-vivo* studies and confocal microscopy experiments as efficient carriers for the dermal and transdermal delivery of highly lipophilic drugs such as DH-CBD and CBD.

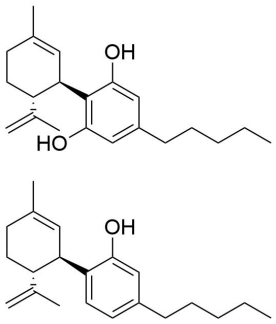

Fig. (1). Chemical structure of cannabidiol (above) and desoxy-cannabidiol (below).

2. MATERIALS AND METHODS

2.1. Materials

Phospholipon 90G was obtained from Lipoid (Ludwigshafen, Germany), Super refined® oleic acid was kindly provided by Croda (Snaith, United Kingdom), and propylene glycol was obtained from Fagron (Rotterdam, The Netherlands). Ethanol absolute anhydrous, R-(+)-limonene, fluorescein isothiocyanate (FITC), and sodium phosphate dibasic dihydrate were purchased from Sigma-Aldrich (Merck KGaA, Darmstadt, Germany). 3-Pentylphenol was purchased from Toronto Research Chemicals (Toronto, Canada). Cannabidiol pure crystals CBD 99one® were kindly provided by Enecta (Amsterdam, The Netherlands). All the other chemical reagents and solvents were purchased from Sigma-Aldrich (Merck KGaA, Darmstadt, Germany), Alfa Aesar (Thermo Fisher Scientific, Kandel, Germany), or Carlo Erba (Milano, Italy). Deuterated solvents for NMR (Merck KGaA, Darmstadt, Germany) had an isotopic purity of a minimum of 99.5%. Fresh 'ultrapure' water (18.2 MΩ, Milli-Q grade) employed for the preparation of all formulations and solutions was produced with the Millipore Milli-Q purification system (MA). Full-thickness porcine skin was obtained by excision of the dorsal area of male or female pig ear skin, kindly provided by the local slaughterhouse F.lli Guerriero (Villafranca Padovana, Italy), and stored at -20°C for up to six months.

2.2. Instruments

NMR spectra were recorded by means of a Bruker 400-AMX spectrometer using tetramethylsilane (TMS) as the internal standard. For each sample, 5 mg were weighed and diluted up to 0.7 mL with deuterated chloroform ($CDCl_3$) into a 5 mm NMR tube. A 90° pulse was calibrated for each sample, and standard NMR parameters were used.

Column chromatography was carried out with silica gel 60 (0.063-0.100 mm, Merck), and elution was performed using the eluent described each time.

2.3. Methods

All the reactions were monitored by thin-layer chromatography (TLC) using the eluent specified for each compound. The TLC was also stained with a vanillin solution prepared as follows: 15 g of

vanillin; 250 mL of 96% ethanol; 2.5 mL of concentrated sulfuric acid.

2.3.1. Synthesis of DH-CBD (1)

2.3.1.1. Synthesis of 2-bromo-4-isopropenyl-1-methylcyclohexanol (3)

R-(+)-Limonene (4.1 g, 30 mmol) was dissolved in a mixture of acetone (15.4 ml) and water (3.4 ml). The mixture was cooled on an ice bath and N-bromosuccinimide (5.9 g, 33.0 mmol) was added in portions over 30 minutes (TLC: CE/EtOAc, 9:1). Acetone was then removed under reduced pressure, and the aqueous layer was diluted with a saturated aqueous solution of $NaHCO_3$. The solution was extracted with ethyl acetate (EtOAc) and the organic layer was dried over anhydrous sodium sulfate (Na_2SO_4). The solvent was removed under reduced pressure to yield 2-bromo-4-isopropenyl-1-methylcyclohexanol (9.5 g, quantitative yield). 1H-NMR ($CDCl_3$-d): 4.76 (d, J = 9.1), 4.20 (s, 1H), 2.48 (s br, 1H), 2.1-1.8 (m, 4H), 1.85 (s, 3H), 1.42 (s, 3H), 1.26 (d, J = 4.7, 1H).

2.3.1.2. Synthesis of (+)-limonene Oxide (4)

A solution of sodium ethoxide (NaOEt) 1M in ethanol (EtOH; 60 ml) was freshly prepared by dissolving metal sodium in previously cooled (ice bath) EtOH. Compound **3** (9.5 g, 30.0 mmol) was dropwise added to NaOEt/EtOH solution while continuously mixing. The reaction was quenched by adding a saturated aqueous solution of ammonium chloride. The solution was extracted with ethyl acetate, the organic layer was dried over Na_2SO_4, and the solvent was evaporated under reduced pressure. The product was purified by distillation at 45°C (10^{-2} mmHg) to yield R-(+)-limonene oxide (3.3 g, yield 73%). 1H-NMR ($CDCl_3$-d): 4.67 (d, J = 1.0, 4H), 2.98 (d, J = 5.3, 1H); 2.07-1.98 (m, 4H), 1.89-1.75 (m, 4H), 1.74-1.60 (m, 2H), 1.66 (s, 3H), 1.31 (s, 3H).

2.3.1.3. Synthesis of (1S,2S,4R)-2-(dimethylamine)-4-isopropenyl-1-methylciclohexanol (5)

4 (32.4 g, 213 mmol) and a 40% dimethylamine aqueous solution (22.7 ml) were mixed and refluxed for 21 hours (TLC: $CHCl_3$/MeOH, 9/1). The mixture was extracted with EtOAc; then the organic phase was washed with a saturated solution of NH_4Cl, dried with anhydrous Na_2SO_4, and filtered. The solvent was removed by rotatory evaporation. The product was purified by column chromatography (eluent: DCM/EtOAc/MeOH/NH_4OH = 70:10:20:1, vanillin stain), thus obtaining (1S,2S,4R)-2-(dimethylamine)-4-isopropenyl-1-methyl-cyclohexanol as a yellow viscous liquid (34.2 g, yield 81%). 1H-NMR ($CDCl_3$-d): 4.91 (d, J = 1.5, 1H), 4.84 (1H, s), 3.52 (s, 1H), 2.47 (dd, J = 13.0, J = 3.4, 1H), 2.35 (m, 1H), 2.24 (s, 6H), 2.05 (ddd; J = 13.5, J = 5.5, J = 2.5, 1H), 1.92 (m, 1H), 1.73 (s, 3H), 1.56-1.41 (m, 4H), 1.21 (s, 3H).

2.3.1.4. Synthesis of (1S,2S,4R)-2-(dimethylamine)-4-isopropenyl-1-methylciclohexanol-N-oxide (6)

5 (1.2 g, 6.1 mmol) was diluted with MeCN (30.5 ml) and water (24.6 ml) and cooled on an ice bath while mixing for 10-15 minutes. Hydrogen peroxide (30% solution, 60.9 mmol) was added dropwise, then the ice bath was removed, and the system was mixed for 2 hours at RT (TLC: $CHCl_3$/MeOH, 75:25). The mixture was cooled in an ice bath, and sodium sulfite (Na_2SO_3, 61.0 mmol) was added. The peroxide was deemed quenched when a colorless solution was obtained when a droplet of the reaction mixture was mixed with a droplet of aqueous sodium iodide. The excess salt was filtered and washed with $CHCl_3$. The filtrate and washings were combined and separated; then the aqueous layer was washed with fresh $CHCl_3$. The organic layers were dried over Na_2SO_4 and the solvent was evaporated under reduced pressure to yield (1S,2S,4R)-2-(dimethylamine)-4-isopropenyl-1-methylciclohexanol-*N*-oxide as an off white solid (1.3 g, quantitative yield). 1H-NMR (CDCl3-d): 5.01 (s, 1H), 4.84 (s, 1H), 3.49 (dd, J = 13.4, J = 3.2, 1H), 3.23 (s, 3H), 3.14 (s, 3H), 2.57 (s, 1H), 2.54 (s, 1H), 2.09 (dq, J = -13.1, J = 5.4, J = 2.5, 1H), 1.94 (m, 1H), 1.77 (ddd, J = -13.3 Hz, J = 13.3, J = 5.3 Hz, 1H), 1.74 (s, 3H), 1.69 (m, 1H), 1.63-1.54 (m, 1H), 1.57 (s, 3H), 1.50 (m, 1H).

2.3.1.5. Synthesis of (1S,4R)-4-isopropenyl-1-methyl-ciclohex-2-en-1-ol (p-mentha-2,8-dien-1-ol; 7)

6 (0.5 g, 2.3 mmol) was heated in a Kugelrohr oven at 120°C under high vacuum (10^{-2} mmHg) until complete pyrolysis of the solid. The colorless distillate was collected with acetone and the solvent was removed under reduced pressure *p*-mentha-2,8-dien-1-ol as a colorless resin (0.32 g, yield 90%). 1H-NMR ($CDCl_3$-d): 5.70 (ddd, J = 10.0, J = 2.4, J = 1.4, 1H), 5.65 (ddd, J = 9.9, J = 2.3, J = 0.8, 1H), 4.78 (q, J = 1.6, 1H), 4.74 (q, J = 0.9, 1H), 2.65 (m, 1H), 1.88-1.73 (m, 2H), 1.73 (s, 3H), 1.66-1.51 (m, 3H), 1.29 (s, 3H).

2.3.1.6. Synthesis of 2-[(1R,6R)-3-methyl-6-(1-methylethenyl)-2-cyclohexen-1-yl]-5-pentylphenol (DH-CBD; 1)

To a solution of **7** (1.5 g, 9.9 mmol) and 3-pentylphenol (1.6 g, 9.9 mmol) in dichloromethane (DCM, 100 ml) was added anhydrous Na_2SO_4 (1.5 g) and the system was purged with nitrogen. The mixture was cooled to -78°C with stirring, then fresh boron trifluoride diethyl etherate ($BF_3 \cdot Et_2O$, 500 µL) was added dropwise, and the reaction was slowly warmed to -10°C over 4 hours (TLC: CE/EtOAc, 80:20). The reaction was quenched with anhydrous sodium carbonate, the salts were filtered, and the filtrate was evaporated by reduced pressure. The final product was purified with the flash chromatography automated system (ISOLERA Biotage) with automatic calculation of elution gradient starting from Rf values obtained from TLC, yielding 2-[(1R,6R)-3-methyl-6-(1-methylethenyl)-2-cyclohexen-1-yl]-5-pentyl-phenol (DH-CBD) as a colorless oil (1.3 g, yield 43%). 1H-NMR ($CDCl_3$-d): 6.87 (d, J = 8.1, 1H), 6.64-6.61 (m, 2H), 5.52 (s, 1H), 5.44 (s, 1H), 4.67 (t, J = 1.7, 1H), 4.56 (s, 1H), 3.40 (m, 1H), 2.51 (t, J = 7.5, 3H), 2.32 (m, 1H), 2.21 (m, 1H), 2.06 (dt, J = 17.7, J = 2.5, 1H), 1.85-1.70 (m, 2H), 1.77 (s, 3H), 1.60-1.55 (m, 2H), 1.59 (s, 3H), 1.37-1.24 (m, 4H), 0.88 (t, J = 6.8, 3H).

2.3.2. Development of Vesicular Systems with Penetration Enhancers

The preparation of vesicles containing different concentrations of PG, OA, or R-(+)-limonene (Limo) was performed with a simple mixing method of two separate phases [12]. Briefly, the phospholipid, the penetration enhancer, and CBD or DH-CBD (0.6-7.0 mg/mL, 0.07-0.8% w/w) were dissolved in ethanol in a well-sealed glass vessel. Then, the aqueous phase was gradually added to the organic phase under vigorous magnetic mixing (1000 rpm). The mixing was continued for additional five minutes, then stored at room temperature in well-sealed glass vessels protected from light. The samples were kept undiluted, in darkness, and at room temperature (20 ± 2°C) for up to 90 days, and their physical appearance, mean particle size and polydispersity were monitored daily to evaluate the shelf life.

Vesicles were prepared with 20-50% w/w EtOH [12, 13], and 2.0-5.0% w/w PC. Penetration enhancers were added at different concentrations: PG higher or equal to the ethanolic content

(20-50% w/w), oleic acid at 0.87 and 0.54 OA:PC molar ratios, and 0.1 to 1% w/w Limo (Table **1**). The influence of a buffered medium as the aqueous phase in OA-containing systems was investigated using 0.1 M phosphate buffer at a pH ≥ 8.

Table 1. Composition of the tested formulations in terms of phosphatidylcholine (PC), ethanol (EtOH), and edge activator (EA) percentages (% w/w).

Formulation	PC (%)	EtOH (%)	EA (%)	Aqueous Phase
PG systems	2.0-5.0	20	PG, 20-50	Water
OA systems	2.0-5.0	20-50	OA, 0.4-0.8	Water or buffer pH 8
Limo systems	2.0-5.0	20-40	Limo, 0.1-1.0	Water

Each preparation was characterized after dilution 1:5 v/v with ultrapure water or 1:500 v/v with equivalent hydroalcoholic solution, in terms of pH and particle size, respectively. The pH was measured with a Five-Easy pH-meter (Mettler Toledo, Switzerland), while Dynamic Light Scattering (DLS) measurements were performed with Malvern Zetasizer NanoZS and Zetasizer Ultra (Malvern Instruments, UK) equipped with a red laser (λ = 633 nm) at a fixed angle of 173°, and analyzed with DTS applications 8.0 or Zetasizer ZS Xplorer 2.1.0 software. Three batches of each system were examined by intensity in triplicate at 25°C under automatically fixed analysis conditions (duration and set position) and monitored for 90 days.

All the combinations of the selected components, reported in Table **1**, were tested for the production of ethosomes or transethosomes. The systems were produced with identical process parameters and evaluated in terms of physical appearance, particle size, polydispersity index, and pH evaluation (in the case of OA systems). Samples with average particle size around or below 300 nm at zero time, and polydispersity index ≤ 0.5 were considered for monitoring the past 30 days. When phase separation phenomena occurred, the samples were excluded from further observation. Optimized formulations, which showed the highest stability over time, were further characterized for their ζ-potential, and the interaction between CBD and the excipients was evaluated with FTIR analyses. The ζ-potential was evaluated on 1:40 dilutions of the formulations in 1:10 diluted PBS buffer (Malvern Zetasizer NanoZS, UK) in folded capillary cells, on three batches of each system. The infrared spectra of the optimized formulations were obtained using the Bruker Tensor 27 FT/IR spectrophotometer. FT-IR spectra, in absorption mode, were collected in a CaF_2 flow cell, with a light path of 56 μm. A total of 128 cumulative scans were performed with a resolution of 4 cm^{-1} in the wavenumber range of 4000-900 cm^{-1}.

2.3.3. Entrapment Efficiency and Release Evaluation

The entrapment efficiency of loaded formulations was evaluated with an in-house optimized dialysis method using equivalent hydroethanolic/glycolic solutions of cannabinoids as a reference. Concentrated formulations (1 mL) were loaded in BioDesignDialysis Tubing™ (BioDesign Inc., ThermoFisher Scientific, USA, 15.5 mm wet diameter, 1.91 mL/cm volume, 14000 Da MWCO), cut into 5 cm length pieces, and hydrated with ultrapure water for 12 hours. The dialysis bag was immersed in 30 mL of an equivalent hydroethanolic (or hydro-glycolic-ethanolic) solution and left stirring for 7 hours. Samples of 1 mL were taken from the media each hour, returning an equal volume of fresh solution, and analyzed by spectrophotometry (UV-Vis Cary® 60, Varian, The Netherlands) using an equivalent hydroethanolic (or glycolic) solution for the baseline correction. The quantification of the free drug concentration was performed using a calibration curve prepared by diluting 1 mg/mL DH-CBD or CBD solutions in EtOH with equivalent hydroethanolic (and glycolic) mixtures, obtaining five standards (2.0-5.0 μg/mL DH-CBD or CBD). The standards were prepared in triplicate before each sample batch analysis, and absorbance peaks at 206 or 202 nm were considered for the quantification of CBD and DH-CBD, respectively. The entrapment efficiency of the vesicular systems was calculated according to equation (1):

$$EE\% = \frac{C_t - C_f}{C_t} \times 100 \quad (1)$$

Where C_t is the total drug concentration, and C_f is the total free drug concentration. C_t was calculated by diluting 40 or 20 μl of the initial formulation (according to the estimated concentration of the cannabinoid) with an equivalent volume of absolute EtOH to disrupt the vesicles, then diluted to 10 mL with a hydroethanolic solution to match the vesicles' dispersion medium, and analyzed by UV detection. The Cf value was set at 7 hours of diffusion.

The release profile of the loaded formulations was evaluated on Franz diffusion cells of 0.64 cm^2 diffusion area and 3.0 mL receptor chamber volume, using a 0.05 μm pore size polycarbonate (PC) membrane (Nucleopore™ Track-Etch membrane, Cytiva, USA), and a 30% v/v hydroethanolic in PBS pH 5.5 as a receiver medium [56, 57]. Each formulation (300 μL) was applied on the donor compartment and samples of 100 μL were withdrawn at predefined intervals over 6 hrs, and an equal amount of fresh receiver solution was returned. The samples were analyzed by UV quantification as described for the entrapment efficiency studies. An equivalent 0.6 mg/mL cannabinoid solution (30% hydroethanolic solution) was used as a control. Data were analyzed with DDSolver free software [58], employing different release models. Once identified the Gompertz model as the most fitting, data were processed accordingly.

2.3.4. Skin Permeation and Retention Evaluation

The *ex-vivo* skin permeation and retention of CBD and DH-CBD from the selected formulations was tested on Franz static diffusion cells (Permegear, Germany, 0.64 cm^2 permeation area, 5.0 mL receptor chamber volume) using porcine ear epidermal membranes prepared by heat separation [59, 60]. Briefly, full-thickness skins were obtained from the local slaughterhouse, removed from the bone with forceps and surgical blades, then stored at -20°C in aluminum foils, sealed in airtight plastic bags, and used within 6 months of storage. The skin integrity up to the conservation time was confirmed by transepidermal water loss (TEWL) measurement with an open chamber device (VapoMeter, Delfin Technologies LtD - Kuopio, Finland). One hour before the experiment, the skin was thawed at room temperature, cut into ~4 cm^2 squares with surgical blades, wrapped in aluminum foil, and heated at 60 ± 1°C in a water bath for 60 seconds. After treatment, the live epidermis and SC were separated from the dermis with surgical blades and forceps, and mounted on the Franz cells keeping the SC on the external side. A 30% v/v hydroethanolic solution was employed as the receiver medium, and full contact with the membrane was carefully assessed. The test was performed under non-occlusive conditions at 32.0 ± 1°C applying 25 μL of each formulation on the epidermal side of the skin. Equivalent solutions of CBD and DH-CBD in 30% EtOH, or 20% EtOH + 40% w/w PG with PG formulations, were applied under the same conditions as controls. Receiver samples of 400 μL were collected at 3 and 6 hrs, stored at -18°C until HPLC analysis and an equal amount of fresh solution was returned.

At the end of the permeation experiments, the skins were washed with 2 × 600 µl of ultrapure water, wiped, and placed in 5 mL of extraction medium (50% v/v ethanolic solution). The skin samples were shaken for 48 hours at 500 rpm (Incubator 1000 orbital shaker, Heidolph, Germany), then mixed in Vortex (60 s) and removed from the tube. The extracts were centrifuged (5000 rpm, 10 min), and the supernatants were collected and stored at -20°C until HPLC analysis.

2.3.5. HPLC Analysis

The quantification of cannabinoids was performed by RP-HPLC on a 1220 Infinity LC (Agilent Technologies, USA) system equipped with DAD detector (λ = 210 nm) and 20 µL loop, adapting a method reported in the literature [61]. A Zorbax 300SB C18 column (4.6 × 250 mm, 100 Å pore size, 5 µm diam.) was used, and the elution was performed under isocratic conditions with MeCN and 50 mM phosphoric acid in water with an 85:15 ratio of MeCN:H_2O, and flux of 1 mL/min. In these conditions, the retention time (R_t) of DH-CBD and CBD were 6.3 min and 3.8 min, respectively. The concentration of both cannabinoids was calculated from calibration curves obtained by dilution of the analyte stock solution 1 mg/mL in EtOH into standard solutions in a range from 12.5 to 100 µg/mL, $R^2 \geq 0.9995$ (Figs. **S1-S3**). Fresh solutions were prepared before each analysis. The total percentage of permeated and accumulated drugs was calculated as the ratio between the penetrated drug amount and the applied drug amount. The applied drug amount was calculated by quantifying the cannabinoids' concentrations in 25 µl of formulation, diluted 1:100 with absolute ethanol.

2.3.6. Skin Depth Imaging by Confocal Laser Scanning Microscopy (CLSM)

OA, PG, and Limo-A formulations containing 0.1% w/w of fluorescein isothiocyanate (FITC) were prepared as described in §2.3.2 by adding the probe in the ethanolic phase. The test was carried out on Franz cells using full-thickness porcine skin and a 30% v/v hydroethanolic solution as a receiver medium under the same conditions described in §2.3.4, using a 0.1% w/w FITC solution in 30% w/w hydroethanolic mixture as a control. Each formulation (25 µL) was applied on the epidermal side of the skin under non-occlusive conditions for 30 minutes, then washed with 2 × 600 µL ultrapure water; the skins were wiped and tape-stripped ten times with adhesive tape. The permeation area was isolated with surgical blades and mounted between two coverslips of 24×60 mm for CLSM examination. An untreated skin sample handled under the same conditions served as a control to rule out the autofluorescence of the skin tissue. Confocal microscopy images were obtained using a Zeiss LSM 800 confocal laser-scanning microscope (Jena, Germany) equipped with a 10× objective (λ_{ex} = 488 nm). Skin samples treated with FITC-loaded systems were observed with increments on the *z*-axis of 9.81 µm, obtaining each *z*-stack image by stitching 5×5 tiles, and quantifying the fluorescence intensity at each *z*-level with ImageJ 1.8.0 software, expressed in arbitrary units.

2.3.7. Statistical Analysis

All samples were prepared in triplicate, and data are shown as the mean of at least three independent experiments. Statistical and bioavailability analyses were performed using two-way analysis of variance (ANOVA) with post-hoc comparisons (Tukey) or the Student's t-test, where appropriate, with $p < 0.05$ as a level of significance (GraphPad Prism software 10.0.2 version - GraphPad Software, CA, USA) (Table **S1**).

3. RESULTS AND DISCUSSION

3.1. Synthesis of DH-CBD

The synthetic pathway was adapted from Wilkinson *et al*. [48] study by improving the formation of the limonene oxide **4** and the subsequent synthesis of compound **5** (Figs. **2a-f**).

Obtaining the correct stereochemistry for intermediate **4** was crucial to improve the overall yield of **1**. For this reason, an enantioselective reaction was employed by using a procedure optimized by Hauenstein *et al*. [62]. Indeed, bromination of **2** with *N*-bromosuccinimide in aqueous medium at low temperature led to **3**. In this way, a 100% *trans*-bromohydrin was obtained with a very high yield [62]. The epoxide **4** was then obtained by treating **3** with the strong base NaOEt.

In this reaction, the alkoxide ion bound to the bromine-linked carbon, causing the leaving of bromine and the subsequent epoxidation.

The addition of another step in the synthetic pathway dramatically improved the reaction yield as compared to the original method (*i.e.*, the direct oxidation with *m*-chloroperbenzoic acid of **2** to **4**), which led to a 1:1 mixture of *cis*- and *trans*-limonene epoxide enantiomers (Figs. **3A**, **B**).

Compound **4** was purified by distillation at 40-60°C and then treated with aqueous dimethylamine under reflux conditions, thus obtaining **5**. In the Wilkinson-Price-Kassiou method, the separation of the *cis*-***5*** and *trans*-***6*** enantiomers by chromatography was difficult to accomplish due to the very similar retention factors of the two compounds. Our improved pathway raised the yield by **5** to 81% against the 35% obtained with the previous method.

After oxidizing **5** with hydrogen peroxide to **6** with a quantitative yield, compound **7** was obtained *via* Cope elimination in the Kugelrohr oven, with a yield over 90%. Although the addition of one extra step, the overall yield of **7** with our strategy was improved from 12% to 48%.

Compound **1** was then obtained by condensation of **7** and 3-pentylphenol with the Lewis acid boron trifluoride. This Friedel-Crafts condensation had to be performed at a very low temperature (-78°C) and a maximum catalyst concentration of 0.5%. These parameters were essential to slow down the reaction kinetics and the high reactivity of BF_3. Thus, the formation of cyclic byproducts and polymerization phenomena were avoided.

3.2. Characterization of Deformable Vesicles and Stability

The influence of each component in the particle size, pH, and entrapment efficiency, at different drug concentrations, was evaluated to assess the best conditions for an efficient encapsulation and transdermal delivery of lipophilic drugs. Optimized vesicles were composed as reported in Table **2** and employed for the *ex-vivo* studies.

3.2.1. Effect on the Particle Size

Vesicular systems prepared with different penetration enhancers were optimized to increase the stability over time and the dermal penetration of the cannabinoids. The influence of each component on the preparation features and stability over time was assessed. In most cases, the preparations showed a characteristic semitransparent appearance, although Limo-containing vesicles resulted in highly opaque dispersions.

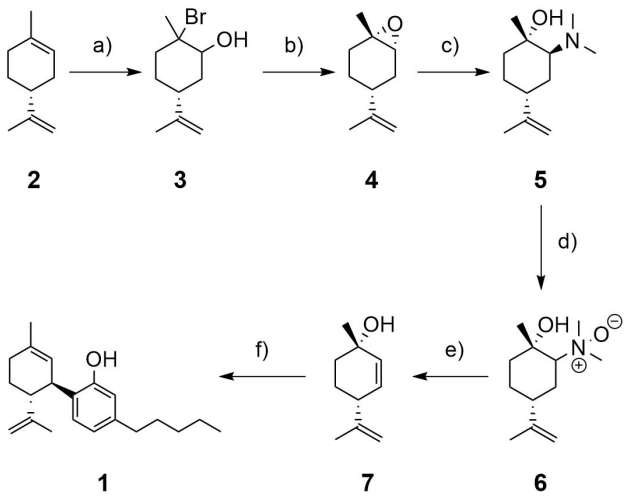

Fig. (2). Improved synthetic pathway of desoxy-CBD. Reagents and conditions: **a**) NBS, H_2O, acetone, 0°C, 30 min, quantitative; **b**) NaOEt, 0°C, distill., 73%; **c**) DMA 40%, refl., 21 h, yield 81%; **d**) H_2O_2, CH_2CN, H_2O, RT, 2 h, quantitative; **e**) 10^{-2} mmHg, 120°C, quantitative; **f**) m-pentylphenol, $BF_3 \cdot Et_2O$, CH_2Cl_2, -78°C, 4h, 26%.

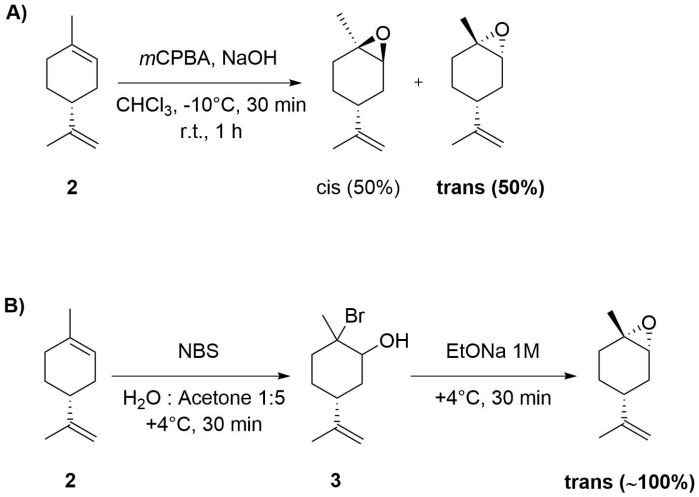

Fig. (3). Schematic representation of *R*-(+)-limonene oxidation by *m*-chloroperbenzoic acid (*m*CPBA) (**A**) and oxidation by introduction of a further step of bromination to the 1-2 unsaturation (**B**). While the oxidation in A) gives an equal mixture of *cis*- and *trans*-diastereomers of R-(+)-limonene epoxide, the introduction of an extra step in B) selectively induces the formation of the *trans*-bromohydrin. This step is followed by quantitative oxidation to *trans*-(+)-limonene epoxide with sodium ethoxide (NaOEt).

Table 2. Optimized formulations with different percentages (%w/w) of phosphatidylcholine (PC), ethanol (EtOH), propylene glycol (PG), limonene (Limo) and 0.6 mg/mL of cannabinoid.

Formulation	PC (%)	EtOH (%)	EA (%)	Aqueous Phase	Drug
PG-1	4.0	20	PG, 40	Water	DH-CBD
PG-2	4.0	20	PG, 40	Water	CBD
OA-1	4.0	30	OA, 0.8*	0.1 M ph. buffer	DH-CBD
OA-2	4.0	30	OA, 0.8*	0.1 ph. buffer	CBD
Limo-1	4.0	25	Limo, 0.25	Water	CBD
Limo-2	5.0	20	Limo, 0.25	Water	CBD

Note: * = OA: PC molar ratio 0.54.

Vesicles containing 3.0 to 5.0% w/w PC showed good physical properties with 30-50% PG, showing superior stability when a 1:10 PC:PG weight ratio was maintained (*e.g.*, 3% PC - 30% PG; 4% PC - 40% PG). In most cases, good nanometric size (90.0-140.0 nm range) and low polydispersion (PDI = 0.3) were achieved. By keeping a fixed percentage of PC (4% w/w), it was observed that an increase in PG concentration led to a general decrease in particle size, as described in the literature [12]. Low PC concentrations (2.0%) could tolerate lower concentrations of PG without showing phase separation (20-30% PG), but the stability over time of these vesicular systems was reduced. Particle size and PDI values were optimally maintained over three months when higher concentrations of PC were used (4-5%). However, an increase in PC concentration caused an increase in the mean particle size. A good balance between particle size and stability over time was achieved with 4% PC and 40% PG systems. A general reduction in the particle size of the vesicles was detected when PG was used as a fluidizing agent, as previously described by several studies [63-65].

OA-containing vesicles showed good nanometric size and polydispersity when 0.54 OA:PC molar ratio was maintained, together with an ethanolic concentration of 30% w/w and a buffered aqueous phase. It is worth noting that the most stable preparations were composed of an OA:PC ratio below the critical ratio of 0.67 reported in the literature for oleic acid in PC bilayers [22]. All the formulations with 2-4% w/w PC showed an overall good PDI ($0.548 \pm 0.160 < PDI < 0.254 \pm 0.195$), although lower lipidic amounts led to higher polydispersity over time. Different amounts of ethanol or higher PC:OA ratios led to phase separation phenomena or polydisperse systems with instability over time. The formulation with the most desirable features was prepared by using a 0.1 M phosphate buffer (pH = 8), showing a mean particle size of 234.1 ± 22.46 nm and PDI of 0.303 ± 0.084, which was maintained over three months (232.0 ± 67.33 nm and PDI 0.434 ± 0.041).

The addition of limonene to the vesicles caused a modification in the systems' appearances from semitransparent to white, fluid dispersions. Vesicles formulated with 0.25% Limo and 4% PC showed overall good stability over at least a week, and the particle size values were maintained in the nanometric size (between 223.7 ± 25.82 and 391.1 ± 28.64 nm). An increase of 10% in ethanolic concentration led to a substantial decrease in the size of almost 200 nm but induced significant instability over one month. However, the instability was mitigated by lowering the PC concentrations. Multiple populations were observed when both high EtOH (≥ 30%) and Limo concentrations were employed, in accordance with the observations of increased size at higher Limo concentrations [9]. Increased mean particle size and precipitation phenomena were observed with 0.5% Limo; 0.25% w/w, together with 4% PC, and 25% EtOH, ensured the highest stability. These results were in agreement with the literature, where the maximum effect of limonene as a 'molecular glue' on a phospholipidic bilayer was reported at a 1:4 terpene:lipid molar ratio [30]. In fact, the most stable formulations were prepared with a 0.29 (Limo-1) or 0.36 (Limo-2) terpene:lipid molar ratio.

3.2.2. Effect on the pH of the Formulation

The pH values of the formulations were assessed, as well. While PG- or Limo-containing vesicles showed more acidic values (around 4.7-4.8 and 6.6-6.8, respectively), OA-containing systems resulted in neutral to slightly basic formulations. This phenomenon could be explained by the apparent pK_a ($pK_{a,app}$) value of fatty acids in an apolar environment. It is well established that vesicular systems composed of PC can include up to 60 mol% of long-chain fatty acids [24, 66], and while the pK_a value of long-chain fatty acids is known to be 4.8 [67, 68], the ionization degree and pH of the fatty acid solutions can affect the apparent value. In equilibrium titration experiments, oleic acid showed an apparent pK_a value of 8.0-8.5, probably due to the formation of a high negative charge density on the surface of lamellar structures and a lowering of the local dielectric constant, thus elevating the $pK_{a,app}$ causing the formation of bilayers and vesicular systems [24]. Similarly, fatty acids incorporated into PC membranes have elevated $pK_{a,app}$ values, around 7.2-7.5, due to the dielectric effect of the non-polar lipid membrane environment [22, 24]. As the hydrophobicity of the environment can highly influence the $pK_{a,app}$ of OA, a change in the pH of the developed formulations was expected to occur. The phenomenon of a pH shifting from slightly basic to slightly acidic in formulations with different OA:PC ratios seemed correlated to the total concentration of OA in the preparations, leading to lower pH at the highest concentration of the fatty acid. Moreover, introducing the drug into the systems likely induced a further increase in the pH values. The presence of a highly hydrophobic drug may have caused an increase in OA $pK_{a,app}$ value. Therefore, the pH value of the preparation resulted in 7.70-7.80, instead of a maximum of 7.5. OA-1 and OA-2 pH values were 7.7 to 7.9, respectively, and were maintained over the entire time of observation.

Both loaded formulations with DH-CBD (OA-1) and CBD (OA-2) showed minor fluctuations in their pH value. In fact, the values obtained were both around 7.7 at zero time, decreased to 7.6 after 30 days, and remained stable for at least three months. This value was maintained only when a buffered aqueous phase was used, either TRIS 10 mM or phosphate buffer 0.1 M, while a progressive decrease towards more acidic values was assessed with ultrapure water.

3.2.3. Effect of the Drug Concentration

The drug concentration affected both vesicles size and stability over time. Higher drug concentrations increased the mean particle size of all the systems, and while all the systems could generally encapsulate drugs up to 7.0 mg/mL, shorter stability over time was observed in Limo-containing systems, as phase separations occurred within a week in formulations with ≥ 1.2 mg/mL CBD. OA-containing vesicles were prepared efficiently with concentrations up to 7.0 mg/mL of DH-CBD, but the systems with the highest amount showed a mean size above 800 nm, unsuitable for efficient transdermal delivery of drugs (Fig. **4**).

PG-containing systems prepared with 4% PC and 40% w/w PG could encapsulate concentrations up to 9 mg/mL DH-CBD, maintaining a mean particle size between 148.2 ± 41.68 nm (zero time) and 111.9 ± 35.81 nm (three months). CBD-loaded systems with up to 9 mg/mL concentrations were tested, but extensive leakage of the drug was recorded (described in §3.2.4).

The best conditions were then achieved by using 4% PC, 20-30% w/w EtOH, and 0.6 mg/mL drug. The vesicular systems thus formulated showed nanometric size suitable for transdermal delivery (between 208.2 ± 20.8 and 321.0 ± 26.32 nm) together with narrow size distribution ($0.184 \pm 0.068 < PDI < 0.387 \pm 0.110$) Their size and PDI were maintained over three months of observation, with a slight decrease registered in OA-2 formulation, as reported in Fig. (**5**).

Moreover, the optimized formulations generally showed a neutral zeta potential (-10.4 ± 1.69 PG-2; -14.8 ± 1.27 Limo-1; -15.9 ± 1.19 Limo-2, respectively), while OA-2 had a negative potential of -44.9 ± 4.34, most likely imparted by oleic acid [69]. FT-IR spectra of the selected formulations were analyzed and compared to the spectra of equivalent empty formulations, as well as to the spectra

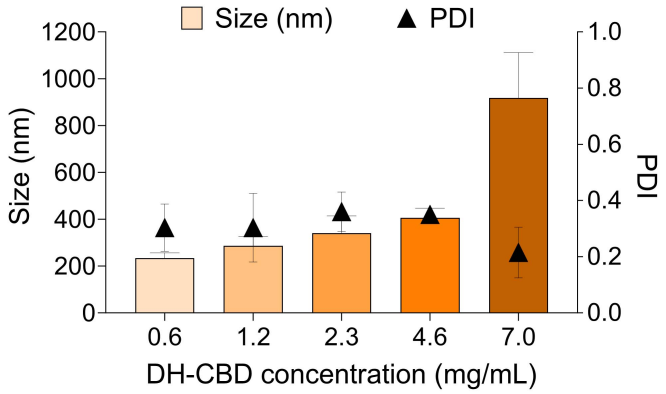

Fig. (4). Mean particle size and polydispersity of OA-containing systems as a function of DH-CBD. Values are expressed as mean ± SD of three independent replicates. (*A higher resolution/colour version of this figure is available in the electronic copy of the article*).

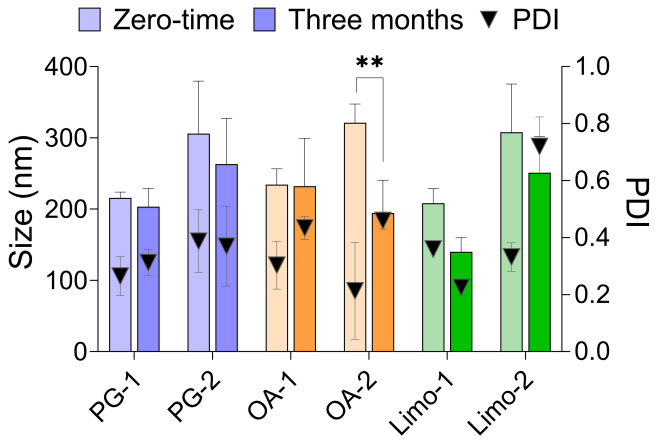

Fig. (5). Mean particle size and polydispersoty of PG-, OA- or Limo-containing vesicles over a period of three months. Values are expressed as mean ± SD of three independent replicates. (*A higher resolution/colour version of this figure is available in the electronic copy of the article*).

of free DH-CBD or CBD in ethanolic solutions. However, the characteristic peaks of ethanol masked most of the signals ascribable to the cannabinoids, except for the peak at 1214 cm^{-1} of DH-CBD and 1204 cm^{-1} of CBD. Nonetheless, FT-IR spectra of each formulation set were coincident, highlighting the lack of the mentioned peaks of the cannabinoids (Fig. **S4**). Thus, it is plausible to assume a drug-excipient interaction due to the mechanical encapsulation of the cannabinoids within the transethosomes.

3.2.4. Effect on the Entrapment Efficiency

Vesicular systems with low PC and high PG amounts showed significant drug leaking, leading to less than 50% entrapment efficiency in 2% PC-containing formulations, especially in CBD-loaded formulations. However, the phenomenon was mitigated by using PG ≤ 40% w/w and 3-4% w/w PC. Under these conditions, the total uptake was assessed above 70% with drug concentrations up to 9 mg/mL, showing the best values with PG-1 and PG-2 (> 85%). All the tested OA- or Limo-containing systems always showed adequate drug retention with both drugs (≥ 80%).

The optimized formulations showed good entrapment efficiency (Fig. **6**).

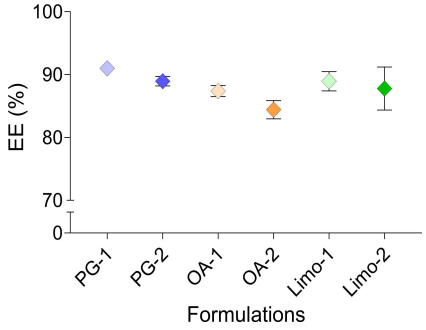

Fig. (6). Drug entrapment efficiency (EE) for each loaded formulation, expressed as mean percentage ± SD of three independent experiments. (*A higher resolution/colour version of this figure is available in the electronic copy of the article*).

The values ranged from 86.0 ± 3.0% to 89.9 ± 1.5% in the case of CBD-containing vesicles, and from 82.3 ± 3.6% to 92.8 ± 0.9% with DH-CBD-containing systems. Although narrow differences could be appreciated between samples, the general trend indicates a slightly higher entrapment efficiency of DH-CBD than CBD.

Release studies did not allow to detect DH-CBD efficiently. However, it was highlighted a slow, abundant diffusion of CBD after 4 hrs (57%), which was completed within the following hour. On the opposite, a sustained release was registered by all the other formulations, in which cumulative percentage was included between 8.8% (Limo-1) and 19.6% (PG-2) after 6 hours (Fig. **S5**). The observed release could be ascribed to the nature of vesicular systems as colloidal carriers, which behave as drug reservoirs, thus acting to release the encapsulated drug in a sustained manner.

3.3. Skin Penetration Studies

3.3.1. Skin Penetration of DH-CBD and CBD

DH-CBD and CBD penetration into the *stratum corneum* and lower layers of the skin is reported in Fig. (**7**).

All the formulations were significantly more efficient in delivering the cannabinoids across the *stratum corneum* ($p<0.05$). Conversely, a simple hydroethanolic solution only showed limited accumulation of DH-CBD and a large depot of CBD in the *stratum corneum*. A detailed description of the permeated amounts is reported in Table **3**. After 3 hours, DH-CBD delivered by OA-1 was below the quantification limit (0.1 µg/mL) in the receptor phase, while it was found in the receptor at 0.2 µg/mL when encapsulated in PG-1. OA-1 and PG-1 increased the total DH-CBD permeation after 6 hours (1.77 ± 0.24 µg/cm^2 and 2.79 ± 0.21 µg/cm^2, respectively), with a 3.9-fold and 2.05-fold increase in the total delivered DH-CBD amount (expressed as µg/cm^2), respectively, as compared to their controls.

Very low drug retention in the membrane was seen in PG-1 treated samples, which in turn showed increased DH-CBD permeability (14.4 ± 0.8%). Delivery into the receptor compartment is often considered an index of transdermal delivery, thus demonstrating the superior capability of these systems to improve the transdermal delivery of DH-CBD. The total delivered DH-CBD dose resulted in 14.4 ± 0.8% and 7.4 ± 1.5% from PG-1 and its control, and 29.2 ± 6.2% and 7.1 ± 1.7% from OA-1 and its control, respectively (Fig. **7A** and Table **3**).

Samples treated with CBD-loaded OA and PG vesicles did not show significant drug permeation after 3 hours of contact, but high permeation rates were assessed after 6 hours (21.06 ± 3.29 and 21.32 ± 4.27 µg/cm^2 from PG-2 and OA-2, respectively; Table **3**). An equivalent cumulative penetration of CBD was assessed between PG-2 and its control solution. However, the control solutions only allowed CBD accumulation on the outmost layers of the skin. At the same time, the formulation reduced the drug skin accumulation and improved the permeation after 6 hours of diffusion. Similar considerations can be made over the Limo-1 and Limo-2 formulations, which significantly improved the skin permeation of CBD after 6 hours, but not its cumulative penetration, as compared to the control. However, OA-2 systems both improved the skin permeation and accumulation of CBD, thus improving the total permeated amount compared to the control solution (Fig. **7B**, Table **3**).

These results suggest the high efficacy of all the systems in delivering cannabinoids to deeper skin layers; PG and Limo-systems reduced CBD retention in the viable epidermis, while OA systems significantly improved the total permeated CBD ($p < 0.0001$) (Figs. **S1-S4**).

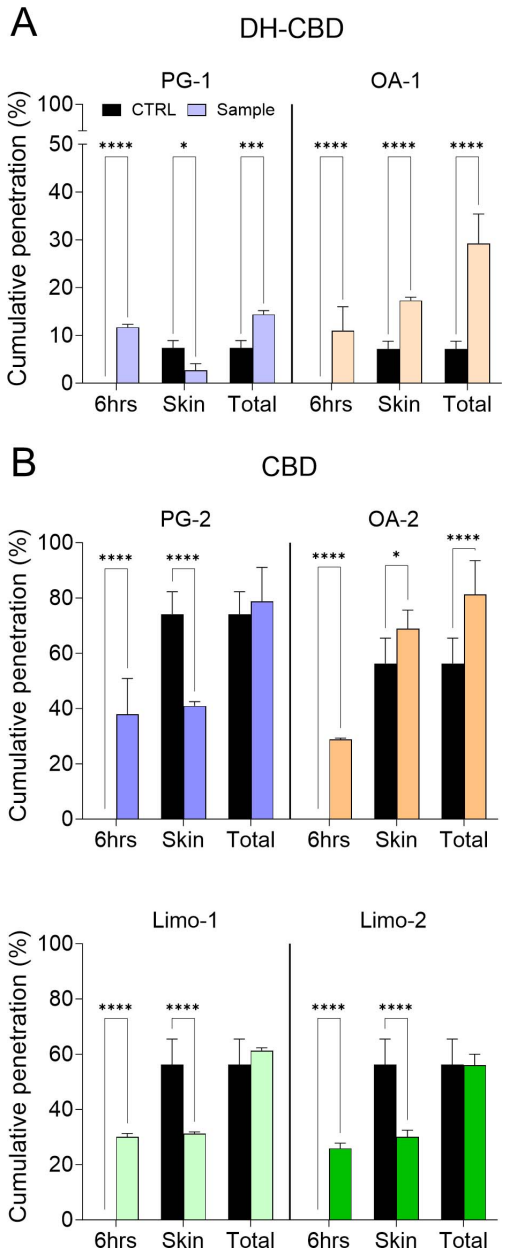

Fig. (7). Cumulative permeated amounts of DH-CBD (**A**) and CBD (**B**), expressed as a percentage of micrograms in each sample (colored bars = formulations; black = control) as compared to the total micrograms applied (mean ± SD, n = 4). (*A higher resolution/-colour version of this figure is available in the electronic copy of the article*).

3.3.2. Skin Depth Imaging

The main pathway for the penetration of most free drugs is believed to be the tortuous intercellular route [70-72]. The results of penetration studies indicate that FITC delivered from OA, PG, and

Table 3. Permeation parameters of CBD and DH-CBD after 6 hrs of diffusion from vesicular systems with propylene glycol (PG), oleic acid (OA), or limonene (Limo), and from hydroethanolic solutions (CTRL) to epidermal porcine skin membranes ('Epid.') (mean ± SD, n = 4 replicates).

Formulation	Applied (μg/cm^2)	Receptor (μg/cm^2)	Epid. (μg/cm^2)	Total Permeat. (μg/cm^2)*	Total Permeat. (%)*
PG-1	24.06	2.79 ± 0.21	0.65 ± 0.33	3.57 ± 0.12	14.4 ± 0.8
CTRL PG-1	23.59	< LOD	1.74 ± 0.35	1.74 ± 0.35	7.4 ± 1.5
PG-2	26.72	10.13 ± 3.47	10.81 ± 0.42	21.06 ± 3.29	78.8 ± 12.3
CTRL PG-2	26.80	< LOD	19.85 ± 2.19	19.85 ± 2.19	74.1 ± 8.2
OA-1	23.58	1.77 ± 0.24	4.72 ± 0.47	7.46 ± 1.31	29.2 ± 6.2
CTRL OA-1	23.59	< LOD	1.91 ± 0.47	1.91 ± 0.47	7.1 ± 1.7
OA-2	26.25	7.56 ± 0.14	17.44 ± 2.45	21.32 ± 4.27	81.2 ± 16.3
Limo-1	26.55	7.99 ± 0.31	8.28 ± 0.19	16.26 ± 0.28	62.7 ± 1.9
Limo-2	27.95	7.24 ± 0.53	8.41 ± 0.67	15.65 ± 1.13	56.6 ± 3.7
CTRL CBD	24.05	< LOD	14.45 ± 3.32	14.45 ± 3.32	56.3 ± 9.2

Note: * = Sum of cannabinoids in the epidermis and the receptor, **Abbreviation**: LOD: limit of detection.

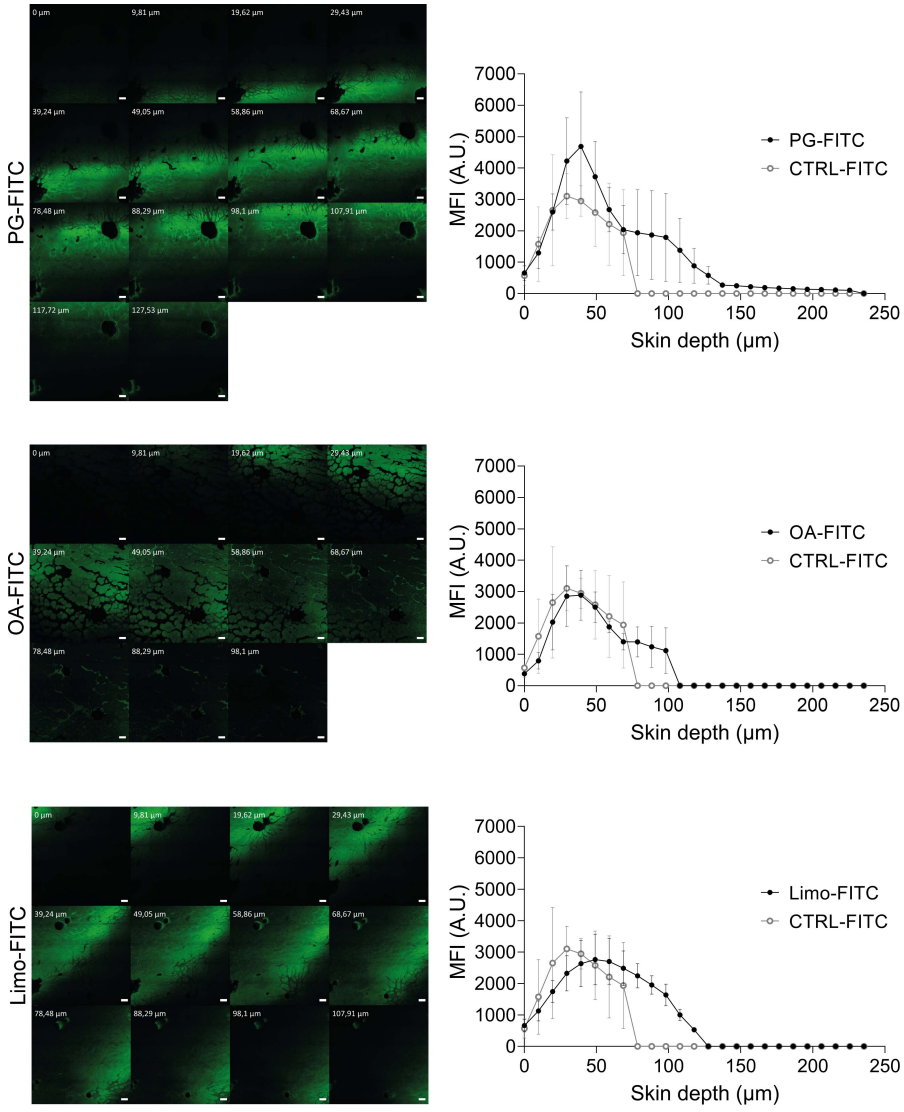

Fig. (8). Skin penetration micrographs (left) of a fluorescent probe (FITC) when delivered by PG-, OA-, or Limo-containing systems. The skin depth reached by FITC, expressed as mean fluorescence intensity (MFI), is reported on the right for each system. All the formulations allowed improved skin depth or fluorescence intensity as compared to the control group. Values are reported as mean ± SEM (n = 3). Scale bar in micrographs: 200 μm. (*A higher resolution/colour version of this figure is available in the electronic copy of the article*).

Limo systems penetrated through various pathways with a tendency to exploit peculiarly the intercellular route, although partial intracellular absorption was observed. This was particularly evident with PG-FITC formulations, while accentuated intracellular fluorescence was assessed with OA-FITC (Fig. **8**).

FITC delivery resulted in increased penetration depth and fluorescence intensity when incorporated into the vesicular systems. In fact, the maximum fluorescence intensity (MaxFI) was reached within 40-50 μm and then dropped rapidly when a hydroethanolic solution of FITC was. On the other hand, the decrease in fluorescence intensity was more gradual from OA-FITC and Limo-FITC formulations. MaxFI values obtained with both groups were assessed around 3000 AU, while a much higher peak (~5000 AU) was detected from samples treated with PG-FITC systems. In terms of depth, the MaxFI using a hydroethanolic solution was reached at 29 μm. Conversely, the fluorescence peak was observed at 40 μm with OA and PG systems, while Limo-FITC showed a MaxFI at 49 μm. While the control samples showed a drop in the fluorescence intensity within 80 μm of skin depth, the signal faded to 0 AU after 240 μm, 110 μm, and 130 μm when the probe was delivered by PG, OA, and Limo systems, respectively, as reported in Fig. (**8**).

These results show how different penetration enhancers in ethosomal-like systems can affect the permeation of the drug by increasing the depth almost 1.5 times, as compared to the control solution. These results were in accordance with the skin permeation experiments since OA systems need more time to permeate, while PG and Limo vesicles are more efficient within shorter times.

By integrating the fluorescence intensity obtained from the samples, a 1.83-fold increase in the skin delivery of the probe was observed with PG-FITC systems, while Limo and OA vesicles increased 1.36 and 1.08 times the skin penetration of the probe, respectively.

CONCLUSION

In this work, innovative systems based on deformable vesicles and three different penetration enhancers - propylene glycol, oleic acid, or limonene, to obtain transethosomes - were prepared and characterized. Moreover, an improved synthesis of a novel synthetic cannabinoid, desoxycannabidiol, was proposed. The drug was successfully synthesized with high purity by reviewing the known literature methods and improving the stereoselectivity in the synthesis of intermediate **4**. Cannabidiol and desoxycannabidiol were loaded in the different developed formulations, leading to vesicles with good nanometric size and stability over at least three months. The drug amount and the penetration enhancers concentration in the systems and the dispersion medium were found to profoundly influence the systems' size and stability. Optimized vesicles were formulated with 20-30% EtOH, 4% PC - 40% PG, 4% PC - 0.8% OA, or 4-5% PC - 0.25% Limo, containing 0.6 mg/mL CBD or DH-CBD. These formulations showed improved skin penetration of both cannabinoids. Confocal microscopy experiments confirmed their superior ability to deliver lipophilic drugs to the deepest layers of the skin. These results suggest the versatility and potential of these carriers for the transdermal delivery of highly lipophilic drugs.

LIST OF ABBREVIATIONS

CBD	=	Cannabidiol
DH-CBD	=	Desoxy-cannabidiol
EA	=	Edge Activator
FITC	=	Fluorescein Isothiocyanate
PC	=	Phosphatidylcholine
PG	=	Propylene Glycol
SC	=	Stratum Corneum

ETHICS APPROVAL AND CONSENT TO PARTICIPATE

Not applicable.

HUMAN AND ANIMAL RIGHTS

Not applicable.

CONSENT FOR PUBLICATION

Not applicable.

AVAILABILITY OF DATA AND MATERIALS

The data supporting the findings of the article is available at https://mega.nz/folder/QjETRTbR#XZIORDsAimJCinY4LHzzQg in the "CPD-Vettorato *et al*. 2023" folder.

FUNDING

This study was supported by the Department of Pharmaceutical and Pharmacological Sciences, University of Padova as Prof. N. Realdon funding; and the Department of Chemistry, University of Padova, as part of the research budget of E. Vettorato's Ph.D. program, XXXII cycle.

CONFLICT OF INTEREST

The authors declare no conflict of interest, financial or otherwise.

ACKNOWLEDGEMENTS

The authors would like to thank the veterinary surgeon Dr. Massimo Marchesan for his support to the research group in the anatomical and histological field, Dr. Andrea Pagetta for his fundamental assistance in the CLSM imaging, Prof. Elka Touitou and Dr. Hiba Natsheh for their outstanding expertise and teachings on ethosomal systems, Dr. Sebastiano Antonio Rizzo for his fundamental support in the release kinetics elaboration, Prof. Paolo Centomo and Tommaso Paravano for the collaboration in the FT-IR analyses.

SUPPLEMENTARY MATERIAL

Supplementary material is available on the publisher's website along with the published article.

REFERENCES

[1] Parnham MJ. Liposome dermatics. In: Braun-Falco O, Korting HC, Maibach HI, Eds. Drug News Perspect. 1991; 4: pp. 567-70. http://dx.doi.org/10.1007/978-3-642-48391-2

[2] Korting HC, Zienicke H, Schäfer-Korting M, Braun-Falco O. Liposome encapsulation improves efficacy of betamethasone dipropionate in atopic eczema but not in psoriasis vulgaris. Eur J Clin Pharmacol 1990; 39(4): 349-51. http://dx.doi.org/10.1007/BF00315408 PMID: 2076716

[3] Mujoriya R, Bodla RB, Dhamande K, Singh D, Patle L. Niosomal drug delivery system: The magic bullet. J Appl Pharm Sci 2011; 1: 20-3.

[4] Souto EB, Macedo AS, Dias-Ferreira J, Cano A, Zielińska A, Matos CM. Elastic and ultradeformable liposomes for transdermal delivery of active pharmaceutical ingredients (Apis). Int J Mol Sci

2021; 22(18): 9743.
http://dx.doi.org/10.3390/ijms22189743 PMID: 34575907
[5] El Maghraby GMM, Williams AC, Barry BW. Skin delivery of oestradiol from deformable and traditional liposomes: Mechanistic studies. J Pharm Pharmacol 2010; 51(10): 1123-34.
http://dx.doi.org/10.1211/0022357991776813 PMID: 10579683
[6] Trotta M, Peira E, Debernardi F, Gallarate M. Elastic liposomes for skin delivery of dipotassium glycyrrhizinate. Int J Pharm 2002; 241(2): 319-27.
http://dx.doi.org/10.1016/S0378-5173(02)00266-1 PMID: 12100859
[7] Trotta M, Peira E, Carlotti ME, Gallarate M. Deformable liposomes for dermal administration of methotrexate. Int J Pharm 2004; 270(1-2): 119-25.
http://dx.doi.org/10.1016/j.ijpharm.2003.10.006 PMID: 14726128
[8] Boinpally RR, Zhou SL, Poondru S, Devraj G, Jasti BR. Lecithin vesicles for topical delivery of diclofenac. Eur J Pharm Biopharm 2003; 56(3): 389-92.
http://dx.doi.org/10.1016/S0939-6411(03)00143-7 PMID: 14602181
[9] Dragicevic-Curic N, Scheglmann D, Albrecht V, Fahr A. Development of liposomes containing ethanol for skin delivery of temoporfin: Characterization and *in vitro* penetration studies. Colloids Surf B Biointerfaces 2009; 74(1): 114-22.
http://dx.doi.org/10.1016/j.colsurfb.2009.07.005 PMID: 19651496
[10] Qadri GR, Ahad A, Aqil M, Imam SS, Ali A. Invasomes of isradipine for enhanced transdermal delivery against hypertension: Formulation, characterization, and *in vivo* pharmacodynamic study. Artif Cells Nanomed Biotechnol 2017; 45(1): 139-45.
http://dx.doi.org/10.3109/21691401.2016.1138486 PMID: 26829018
[11] Opatha SAT, Titapiwatanakun V, Chutoprapat R. Transfersomes: A promising nanoencapsulation technique for transdermal drug delivery. Pharmaceutics 2020; 12(9): 855.
http://dx.doi.org/10.3390/pharmaceutics12090855 PMID: 32916782
[12] Touitou E, Dayan N, Bergelson L, Godin B, Eliaz M. Ethosomes - novel vesicular carriers for enhanced delivery: Characterization and skin penetration properties. J Control Release 2000; 65(3): 403-18.
http://dx.doi.org/10.1016/S0168-3659(99)00222-9 PMID: 10699298
[13] Touitou E. Composition for applying substances to or through the skin. US Patent 5540934A, 1998.
[14] Song CK, Balakrishnan P, Shim CK, Chung SJ, Chong S, Kim DD. A novel vesicular carrier, transethosome, for enhanced skin delivery of voriconazole: Characterization and *in vitro/in vivo* evaluation. Colloids Surf B Biointerfaces 2012; 92: 299-304.
http://dx.doi.org/10.1016/j.colsurfb.2011.12.004 PMID: 22205066
[15] Ainbinder D, Touitou E. A new approach for skin tumor treatment: From delivery system characterization to *in vivo* evaluation. Drug Deliv Transl Res 2011; 1(1): 53-65.
http://dx.doi.org/10.1007/s13346-010-0006-y PMID: 25787889
[16] Verma S, Utreja P. Vesicular nanocarrier based treatment of skin fungal infections: Potential and emerging trends in nanoscale pharmacotherapy. Asian J Pharm Sci 2019; 14(2): 117-29.
http://dx.doi.org/10.1016/j.ajps.2018.05.007 PMID: 32104444
[17] Manconi M, Mura S, Sinico C, Fadda AM, Vila AO, Molina F. Development and characterization of liposomes containing glycols as carriers for diclofenac. Colloids Surf A Physicochem Eng Asp 2009; 342(1-3): 53-8.
http://dx.doi.org/10.1016/j.colsurfa.2009.04.006
[18] Abdulbaqi IM, Darwis Y, Khan NAK, Assi RA, Khan AA. Ethosomal nanocarriers: The impact of constituents and formulation techniques on ethosomal properties, *in vivo* studies, and clinical trials. Int J Nanomedicine 2016; 11: 2279-304.
http://dx.doi.org/10.2147/IJN.S105016 PMID: 27307730
[19] Williams AC, Barry BW. Penetration enhancers. Adv Drug Deliv Rev 2012; 64: 128-37.
http://dx.doi.org/10.1016/j.addr.2012.09.032 PMID: 15019749
[20] Touitou E, Fabin B. Altered skin permeation of a highly lipophilic molecule: Tetrahydrocannabinol. Int J Pharm 1988; 43(1-2): 17-22.
http://dx.doi.org/10.1016/0378-5173(88)90053-1
[21] Goodman M, Barry BW. Action of penetration enhancers on human skin as assessed by the permeation of model drugs 5-fluorouracil and estradiol. I. Infinite dose technique. J Invest Dermatol 1988; 91(4): 323-7.
http://dx.doi.org/10.1111/1523-1747.ep12475655 PMID: 3171212
[22] Ptak M, Egret-Charlier M, Sanson A, Bouloussa O. A NMR study of the ionization of fatty acids, fatty amines and N-acylamino acids incorporated in phosphatidylcholine vesicles. Biochim Biophys Acta Biomembr 1980; 600(2): 387-97.
http://dx.doi.org/10.1016/0005-2736(80)90442-3 PMID: 7407120
[23] Zakir F, Vaidya B, Goyal AK, Malik B, Vyas SP. Development and characterization of oleic acid vesicles for the topical delivery of fluconazole. Drug Deliv 2010; 17(4): 238-48.
http://dx.doi.org/10.3109/10717541003680981 PMID: 20235758
[24] Cistola DP, Hamilton JA, Jackson D, Small DM. Ionization and phase behavior of fatty acids in water: Application of the Gibbs phase rule. Biochemistry 1988; 27(6): 1881-8.
http://dx.doi.org/10.1021/bi00406a013 PMID: 3378036
[25] El Maghraby GMM, Williams AC, Barry BW. Oestradiol skin delivery from ultradeformable liposomes: Refinement of surfactant concentration. Int J Pharm 2000; 196(1): 63-74.
http://dx.doi.org/10.1016/S0378-5173(99)00441-X PMID: 10675708
[26] El Maghraby GMM, Williams AC, Barry BW. Interactions of surfactants (edge activators) and skin penetration enhancers with liposomes. Int J Pharm 2004; 276(1-2): 143-61.
http://dx.doi.org/10.1016/j.ijpharm.2004.02.024 PMID: 15113622
[27] Shamma RN, Elsayed I. Transfersomal lyophilized gel of buspirone HCl: Formulation, evaluation and statistical optimization. J Liposome Res 2013; 23(3): 244-54.
http://dx.doi.org/10.3109/08982104.2013.801489 PMID: 23713516
[28] Srisuk P, Thongnopnua P, Raktanonchai U, Kanokpanont S. Physico-chemical characteristics of methotrexate-entrapped oleic acid-containing deformable liposomes for *in vitro* transepidermal delivery targeting psoriasis treatment. Int J Pharm 2012; 427(2): 426-34.
http://dx.doi.org/10.1016/j.ijpharm.2012.01.045 PMID: 22310459
[29] Choi J, Choi MK, Chong S, Chung SJ, Shim CK, Kim DD. Effect of fatty acids on the transdermal delivery of donepezil: *In vitro* and *in vivo* evaluation. Int J Pharm 2012; 422(1-2): 83-90.
http://dx.doi.org/10.1016/j.ijpharm.2011.10.031 PMID: 22037444
[30] Witzke S, Duelund L, Kongsted J, Petersen M, Mouritsen OG, Khandelia H. Inclusion of terpenoid plant extracts in lipid bilayers investigated by molecular dynamics simulations. J Phys Chem B 2010; 114(48): 15825-31.
http://dx.doi.org/10.1021/jp108675b PMID: 21070035
[31] Šturm L, Poklar Ulrih N. Propolis flavonoids and terpenes, and their interactions with model lipid membranes: A review. Adv Biomembr Lipid Self-Assem 2020; 32: 25-52.
http://dx.doi.org/10.1016/bs.abl.2020.04.003
[32] Cornwell PA, Barry BW, Bouwstra JA, Gooris GS. Modes of action of terpene penetration enhancers in human skin; Differential scanning calorimetry, small-angle X-ray diffraction and enhancer uptake studies. Int J Pharm 1996; 127(1): 9-26.
http://dx.doi.org/10.1016/0378-5173(95)04108-7
[33] Touitou E, Natsheh H. Topical administration of drugs incorporated in carriers containing phospholipid soft vesicles for the treatment of skin medical conditions. Pharmaceutics 2021; 13(12): 2129.
http://dx.doi.org/10.3390/pharmaceutics13122129 PMID: 34959410
[34] Lodzki M, Godin B, Rakou L, Mechoulam R, Gallily R, Touitou E. Cannabidiol-transdermal delivery and anti-inflammatory effect in a murine model. J Control Release 2003; 93(3): 377-87.
http://dx.doi.org/10.1016/j.jconrel.2003.09.001 PMID: 14644587
[35] Natsheh H, Vettorato E, Touitou E. Ethosomes for dermal administration of natural active molecules. Curr Pharm Des 2019; 25(21): 2338-48.
http://dx.doi.org/10.2174/1381612825666190716095826 PMID: 31333087
[36] Abrams DI. The therapeutic effects of Cannabis and cannabinoids:

An update from the National Academies of Sciences, Engineering and Medicine report. Eur J Intern Med 2018; 49: 7-11. http://dx.doi.org/10.1016/j.ejim.2018.01.003 PMID: 29325791

[37] Devinsky O, Cross JH, Laux L, *et al.* Trial of cannabidiol for drug-resistant seizures in the dravet syndrome. N Engl J Med 2017; 376(21): 2011-20. http://dx.doi.org/10.1056/NEJMoa1611618 PMID: 28538134

[38] Upadhya D, Castro OW, Upadhya R, Shetty AK. Prospects of cannabidiol for easing status epilepticus-induced epileptogenesis and related comorbidities. Mol Neurobiol 2018; 55(8): 6956-64. http://dx.doi.org/10.1007/s12035-018-0898-y PMID: 29372545

[39] Xiong W, Cheng K, Cui T, *et al.* Cannabinoid potentiation of glycine receptors contributes to cannabis-induced analgesia. Nat Chem Biol 2011; 7(5): 296-303. http://dx.doi.org/10.1038/nchembio.552 PMID: 21460829

[40] Hejazi N, Zhou C, Oz M, Sun H, Ye JH, Zhang L. Delta9-tetrahydrocannabinol and endogenous cannabinoid anandamide directly potentiate the function of glycine receptors. Mol Pharmacol 2006; 69(3): 991-7. http://dx.doi.org/10.1124/mol.105.019174 PMID: 16332990

[41] Ahrens J, Demir R, Leuwer M, *et al.* The nonpsychotropic cannabinoid cannabidiol modulates and directly activates alpha-1 and alpha-1-Beta glycine receptor function. Pharmacology 2009; 83(4): 217-22. http://dx.doi.org/10.1159/000201556 PMID: 19204413

[42] Xiong W, Wu X, Lovinger DM, *et al.* A common molecular basis for exogenous and endogenous cannabinoid potentiation of glycine receptors. J Neurosci 2012; 32(15): 5200-8. http://dx.doi.org/10.1523/JNEUROSCI.6347-11.2012 PMID: 22496565

[43] Xiong W, Cui T, Cheng K, *et al.* Cannabinoids suppress inflammatory and neuropathic pain by targeting α3 glycine receptors. J Exp Med 2012; 209(6): 1121-34. http://dx.doi.org/10.1084/jem.20120242 PMID: 22585736

[44] Petrzilka T, Haefliger W, Sikemeier C. Synthese von Haschisch-Inhaltsstoffen. 4. Mitteilung. Helv Chim Acta 1969; 52(4): 1102-34. http://dx.doi.org/10.1002/hlca.19690520427

[45] Reggio PH, Bramblett RD, Yuknavich H, *et al.* The design, synthesis and testing of desoxy-CBD: Further evidence for a region of steric interference at the cannabinoid receptor. Life Sci 1995; 56(23-24): 2025-32. http://dx.doi.org/10.1016/0024-3205(95)00185-9 PMID: 7776828

[46] Schenck GO, Neumüller OA, Ohloff G, Schroeter S. Zur Autoxydation des (+)-Limonens. Justus Liebigs Ann Chem 1965; 687(1): 26-39. http://dx.doi.org/10.1002/jlac.19656870105

[47] Rickards RW, Watson WP. Conversion of (+)-(R)-Limonene into (+)-(1S,4R)-p-mentha-2,8-dien-1-ol, an intermediate in the synthesis of tetrahydrocannabinoids. Aust J Chem 1980; 33(2): 451-4. http://dx.doi.org/10.1071/CH9800451

[48] Wilkinson SM, Price J, Kassiou M. Improved accessibility to the desoxy analogues of Δ9-tetrahydrocannabinol and cannabidiol. Tetrahedron Lett 2013; 54(1): 52-4. http://dx.doi.org/10.1016/j.tetlet.2012.10.080

[49] Baron EP. Comprehensive review of medicinal marijuana, cannabinoids, and therapeutic implications in medicine and headache: What a long strange trip it's been. Headache 2015; 55(6): 885-916. http://dx.doi.org/10.1111/head.12570 PMID: 26015168

[50] National Academies of Sciences, Medicine Division, Board on Population Health, Public Health Practice, Committee on the Health Effects of Marijuana, An Evidence Review, Research Agenda. The health effects of cannabis and cannabinoids: The current state of evidence and recommendations for research. 2017; pp. 440. http://dx.doi.org/10.17226/24625

[51] National Center for Biotechnology Information. Pubchem compound summary for CID 50919314, 5-Desoxy-delta9-tetrahydrocannabinol. 2022. Available from: https://pubchem.ncbi.nlm.nih.gov/compound/5-Desoxy-delta9-tetrahydrocannabinol (Accessed March 13, 2022).

[52] Barry BW. Novel mechanisms and devices to enable successful transdermal drug delivery. Eur J Pharm Sci 2001; 14(2): 101-14. http://dx.doi.org/10.1016/S0928-0987(01)00167-1

[53] Lazzari P, Fadda P, Marchese G, Casu GL, Pani L. Antinociceptive activity of Δ9-tetrahydrocannabinol non-ionic microemulsions. Int J Pharm 2010; 393(1-2): 239-44. http://dx.doi.org/10.1016/j.ijpharm.2010.04.010 PMID: 20399844

[54] Murgia S, Fadda P, Colafemmina G, *et al.* Characterization of the Solutol® HS15/water phase diagram and the impact of the Δ9-tetrahydrocannabinol solubilization. J Colloid Interface Sci 2013; 390(1): 129-36. http://dx.doi.org/10.1016/j.jcis.2012.08.068 PMID: 23099249

[55] Hammell DC, Zhang LP, Ma F, *et al.* Transdermal cannabidiol reduces inflammation and pain-related behaviours in a rat model of arthritis. Eur J Pain 2016; 20(6): 936-48. http://dx.doi.org/10.1002/ejp.818 PMID: 26517407

[56] Tai K, Rappolt M, He X, *et al.* Effect of β-sitosterol on the curcumin-loaded liposomes: Vesicle characteristics, physicochemical stability, *in vitro* release and bioavailability. Food Chem 2019; 293: 92-102. http://dx.doi.org/10.1016/j.foodchem.2019.04.077 PMID: 31151654

[57] Abd El-Alim SH, Kassem AA, Basha M, Salama A. Comparative study of liposomes, ethosomes and transfersomes as carriers for enhancing the transdermal delivery of diflunisal: *In vitro* and *in vivo* evaluation. Int J Pharm 2019; 563: 293-303. http://dx.doi.org/10.1016/j.ijpharm.2019.04.001 PMID: 30951860

[58] Zhang Y, Huo M, Zhou J, *et al.* DDSolver: An add-in program for modeling and comparison of drug dissolution profiles. AAPS J 2010; 12(3): 263-71. http://dx.doi.org/10.1208/s12248-010-9185-1 PMID: 20373062

[59] Godin B, Touitou E. Transdermal skin delivery: Predictions for humans from *in vivo*, *ex vivo* and animal models. Adv Drug Deliv Rev 2007; 59(11): 1152-61. http://dx.doi.org/10.1016/j.addr.2007.07.004 PMID: 17889400

[60] Casiraghi A, Musazzi UM, Centin G, Franzè S, Minghetti P. Topical administration of cannabidiol: Influence of vehicle-related aspects on skin permeation process. Pharmaceuticals 2020; 13(11): 337. http://dx.doi.org/10.3390/ph13110337 PMID: 33114270

[61] Burnier C, Esseiva P, Roussel C. Quantification of THC in cannabis plants by fast-HPLC-DAD: A promising method for routine analyses. Talanta 2019; 192: 135-41. http://dx.doi.org/10.1016/j.talanta.2018.09.012 PMID: 30348368

[62] Hauenstein O, Reiter M, Agarwal S, Rieger B, Greiner A. Bio-based polycarbonate from limonene oxide and CO_2 with high molecular weight, excellent thermal resistance, hardness and transparency. Green Chem 2016; 18(3): 760-70. http://dx.doi.org/10.1039/C5GC01694K

[63] Elmoslemany RM, Abdallah OY, El-Khordagui LK, Khalafallah NM. Propylene glycol liposomes as a topical delivery system for miconazole nitrate: Comparison with conventional liposomes. AAPS PharmSciTech 2012; 13(2): 723-31. http://dx.doi.org/10.1208/s12249-012-9783-6 PMID: 22566173

[64] Zhang JP, Wei YH, Zhou Y, Li YQ, Wu XA. Ethosomes, binary ethosomes and transfersomes of terbinafine hydrochloride: A comparative study. Arch Pharm Res 2012; 35(1): 109-17. http://dx.doi.org/10.1007/s12272-012-0112-0 PMID: 22297749

[65] Natsheh H, Touitou E. Phospholipid vesicles for dermal/transdermal and nasal administration of active molecules: The effect of surfactants and alcohols on the fluidity of their lipid bilayers and penetration enhancement properties. Molecules 2020; 25(13): 2959. http://dx.doi.org/10.3390/molecules25132959 PMID: 32605117

[66] Mabrey S, Sturtevant JM. Incorporation of saturated fatty acids into phosphatidylcholine bilayers. Biochim Biophys Acta Lipids Lipid Metab 1977; 486(3): 444-50. http://dx.doi.org/10.1016/0005-2760(77)90094-7 PMID: 856286

[67] Cistola DP, Small DM, Hamilton JA. Ionization behavior of aqueous short-chain carboxylic acids: A carbon-13 NMR study. J Lipid Res 1982; 23(5): 795-9. http://dx.doi.org/10.1016/S0022-2275(20)38114-1 PMID: 7119577

[68] Cistola DP, Small DM, Hamilton JA. Carbon ^{13}NMR studies of sat-

urated fatty acids bound to bovine serum albumin. II. Electrostatic interactions in individual fatty acid binding sites. J Biol Chem 1987; 262(23): 10980-5.
http://dx.doi.org/10.1016/S0021-9258(18)60914-7 PMID: 3611100

[69] Bruno MC, Gagliardi A, Mancuso A, *et al.* Oleic acid-based vesicular nanocarriers for topical delivery of the natural drug thymoquinone: Improvement of anti-inflammatory activity. J Control Release 2022; 352: 74-86.
http://dx.doi.org/10.1016/j.jconrel.2022.10.011 PMID: 36228953

[70] Schaefer H, Redelmeier TE. Skin barrier: Principles of percutaneous absorption. Basel, New York: Karger 1996.

[71] Maibach H. Dermatological formulations: Percutaneous absorption. By Brian W. Barry. Marcel Dekker, 270 Madison Avenue, New York, NY 10016. 1983. 479pp. 16 × 23.5cm. Price $55.00 (2070 higher outside the US. and Canada). J Pharm Sci 1984; 73(4): 573.
http://dx.doi.org/10.1002/jps.2600730442

[72] Touitou E. Drug delivery across the skin. Expert Opin Biol Ther 2002; 2(7): 723-33.
http://dx.doi.org/10.1517/14712598.2.7.723 PMID: 12387671